THE JOURNAL OF PHYSICAL CHEMISTRY A

Article

pubs.acs.org/JPCA

Excitation Spectra of Cation and Anion Radicals of Several Unsaturated Hydrocarbons: Symmetry Adapted Cluster-Configuration Interaction Theoretical Study

Yasushi Honda,[†,∥] Tadamasa Shida,[‡] and Hiroshi Nakatsuji*[,†,§]

[†]Quantum Chemistry Research Institute (QCRI), JST-CREST, 1-36 Goryo-Oohara, Nishikyo-ku, Kyoto 615-8245, Japan

[‡]Department of Chemistry, Faculty of Science, Kyoto University, Kitashirakawa-Oiwakecho, Sakyo-ku, Kyoto 606-8502, Japan

[§]Institute of Multidisciplinary Research for Advanced Materials (IMRAM), Tohoku University, 2-1-1 Katahira, Aoba-ku, Sendai 980-8577, Japan

Supporting Information

ABSTRACT: Excitation spectra of cation and anion radicals of unsaturated hydrocarbons, hexatriene[±], octatetraene[±], cyclopentadiene[+], 1,3-cyclohexadiene[+], and naphthalene[±], were studied by the symmetry adapted cluster-configuration interaction (SAC-CI) method. The calculated results reasonably reproduced the experimental spectra observed by one of the authors (T.S.) and gave reasonable assignments. The two bands observed in the experimental spectra were assigned to $\pi-\pi_{SOMO}$ and $\pi_{SOMO}-\pi^*$ for the cation radicals and $\pi^*_{SOMO}-\pi^*$ and $\pi-\pi^*_{SOMO}$ for the anion radicals, in order of increasing energy, except for naphthalene[±]. The four bands of naphthalene[+] originated from $\pi-\pi_{SOMO}$, $\pi-\pi_{SOMO}$, $\pi_{SOMO}-\pi^*$, and $\pi_{SOMO}-\pi^*$ and those of naphthalene[−] originated from $\pi^*_{SOMO}-\pi^*$, $\pi^*_{SOMO}-\pi^*$, $\pi-\pi^*_{SOMO}$, $\pi^*_{SOMO}-v\pi^*$, and $\pi-\pi^*_{SOMO}$, in order of increasing energy. The SOMO orbitals were involved in the intense bands of both cation and anion radicals. Moreover, the ionization energies (IEs) and electron affinities (EAs) of these hydrocarbons were in good agreement with the experimental values, whereas the EAs of hexatriene and octatetraene were predicted to be negative and positive, respectively. The calculated IE + EA values were nearly constant for the three $\pi-\pi^*$ pairing states of hexatriene[±], octatetraene[±], and naphthalene[±], indicating that the pairing theorem is valid even at the SAC-CI level.

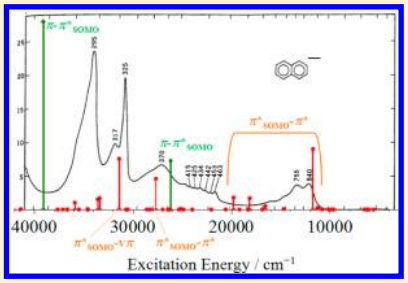

1. INTRODUCTION

Excited states of conjugated polyenes have been studied intensively both experimentally and theoretically (see ref 1, for example) because of their fundamental and industrial advantages.[2−7] Their cation and anion radicals, which exhibit open-shell electronic structures, are also important; for example, some polycyclic aromatic hydrocarbon cations are considered strong candidates as carriers in diffuse interstellar absorption bands and are thought to be the source of various interstellar infrared emission features in certain energy ranges.[2,3] The excitation spectra of cation and anion radicals have not been studied to the same extent as those of neutral molecules owing to their instability. However, two decades ago, one of the authors developed an experimental method for observing the absorption spectra of cation and anion radicals trapped in glassy organic matrices and reported the experimental absorption spectra for various radical cations and anions.[8] In the gas phase, the electronic structures of molecular cations were studied experimentally by photoelectron spectroscopy[9,10] and those of molecular anions by electron transmission spectroscopy (ETS).[11] In the present study, we examine the cation/anion radicals shown in Figure 1. All of these radicals have been studied experimentally by Shida in frozen solutions.[8] In addition, gas-phase experiments have been reported for the hexadiene cation,[12−15] octatetraene cation,[14,16] cyclopentadiene cation,[17] 1,3-cyclohexadiene cation,[18] naphthalene cation,[19−28] hexadiene anion,[29] octatetraene anion,[30] and naphthalene anion.[31−38]

The absorption spectra of open-shell radicals are usually interpreted and assigned on the basis of Koopmans' concept[39] of orbitals. Figure 2 illustrates the electronic structures of the ground and excited states of open-shell doublet states. These excitation states are grouped into three types. Type I is the state in which the main configuration is represented by the promotion of an electron from the SOMO to one of the higher unoccupied orbitals. Type II is the state produced by electron promotion to the SOMO from one of the lower doubly occupied orbitals. Type III is the state produced by electron promotion from a doubly occupied orbital to an unoccupied orbital. As expected, lower-energy absorptions are usually due to type I (from SOMO to LUMO) and type II (from HOMO to SOMO) excitations, and the intensities of these absorptions are usually strong because they result from excitations between two sequential MOs, which differ symmetrically by a single node. On the other hand, type III excitations are usually higher in energy because even the lowest

Received: May 28, 2012
Revised: November 7, 2012
Published: November 15, 2012

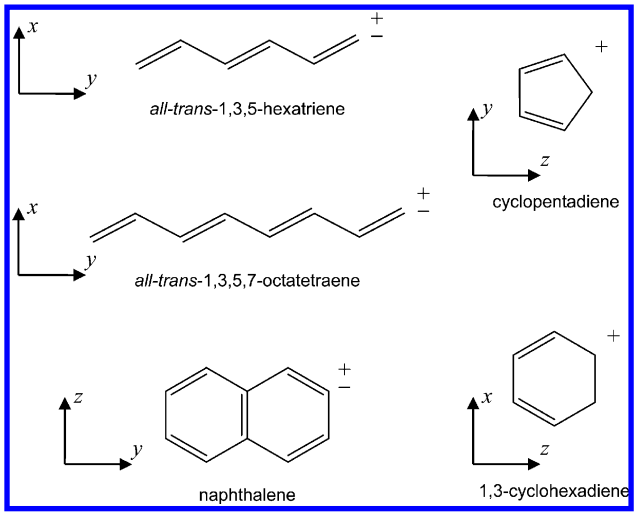

Figure 1. Target cation/anion radicals for the SAC-CI calculations.

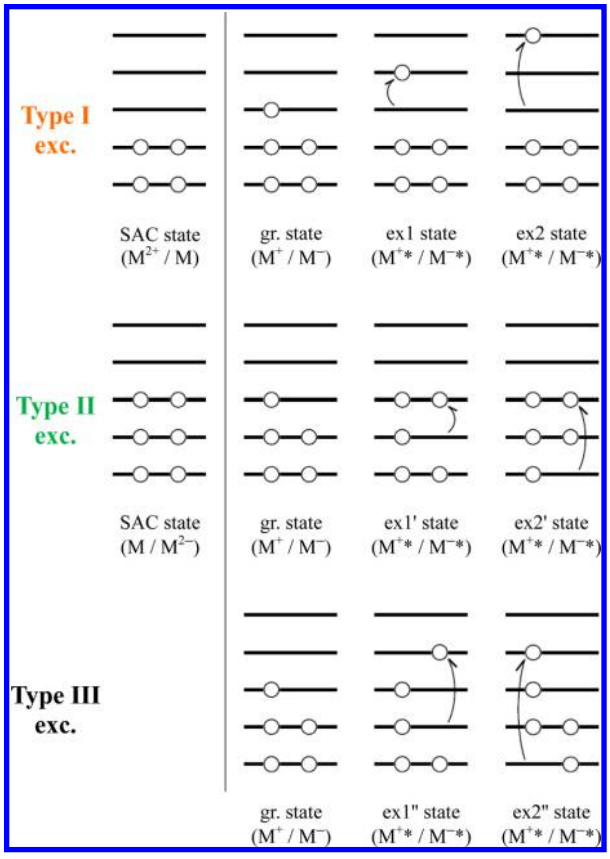

Figure 2. Three types of excitations for the cation/anion radicals.

excitation involves a transition between "nonsequential" orbitals, and thus, their intensities are often weak.

The pairing theorem,[35,40−46] which interconnects the electronic structures of cation and anion pairs, is a significant theorem for studying both cation and anion radicals produced from the same neutral species. This theorem represents the hydrocarbons that have alternant structure; all the hydrocarbons studied in this paper (Figure 1) are alternant hydrocarbons. According to this theorem, the sum of the ionization energy (IE) and electron affinity (EA) is expected to be a constant for the π_n−π_n* (n = 1, 2, ...) orbital pairs. However, this theorem is valid only with the Hückel- and Pariser−Parr−Pople (PPP)-type molecular orbital theories. It also does not consider the geometry relaxations accompanying ionizations and electron attachments, although sometimes the adiabatic values are discussed. Allan et al. noted that the (IE + EA)/2 values were nearly constant for linear polyenes (ethylene, butadiene, hexatriene, and octatetraene) in their analysis.[30] Staley and Strnad also analyzed Hartree−Fock orbital energies of the polyenes with small basis sets and obtained similar results.[40] However, it is unknown whether this theorem is satisfied by accurate calculations at the state-of-the-art level.

To provide reliable theoretical analysis and spectral assignments, we used the symmetry adapted cluster (SAC) method[47] for closed-shell states and the SAC-configuration interaction (SAC-CI) method[48,49] for doublet states. SAC/SAC-CI is a powerful methodology including electron correlations and can describe not only closed-shell but also open-shell electronic states of various spin multiplicities. This theory has a long history of theoretical developments[50,51] and applications to various fields, such as fine spectroscopy,[52−55] photobiology,[56−61] and molecular engineering.[62−64] Furthermore, the SAC/SAC-CI method is readily applicable to the study of doublet-to-doublet excitation spectra:[65,66] both ground and excited states are calculated with the SAC-CI method starting from the appropriate closed-shell states of the molecule. In this study, we investigated the ground and excited states of the cation and anion doublet radicals of several unsaturated hydrocarbons: hexatriene$^{\pm}$, octatetraene$^{\pm}$, cyclopentadiene^{+}, 1,3-cyclohexadiene^{+}, and naphthalene$^{\pm}$. The calculated results showed reasonable agreement with the experimental observations, which will provide the basis for the succeeding theoretical analyses to obtain insight into the natures lying behind the observed phenomena.

2. COMPUTATIONAL METHOD

The geometries of the target cation and anion radicals, shown in Figure 1, were optimized using the UB3LYP DFT method with the D95(d,p) basis set of the standard scaling factors,[67] which has a double-ζ + polarization(d,p) quality, together with Dunning's diffuse anion basis[68] for the carbon atoms. The ground and excited states of the target radicals were calculated with the SAC/SAC-CI SD-*R* method, in which one- and two-electron excitation operators were considered as linked operators relative to the reference closed-shell state. We first calculated the ROHF orbitals of each radical used as reference orbitals in the SAC/SAC-CI calculations. Then, we calculated the appropriate closed-shell state (neutral, dication, or dianion state) with the SAC method and the open-shell cation or anion states (both ground and excited states) with the SAC-CI method. The type I states were calculated by the SAC-CI electron attachment method, and the type II states, by the SAC-CI electron ionization procedure based on the SAC method irrespective of whether the actual molecule was a cation or an anion. All calculations were carried out using the Gaussian 09 program packages.[69] The 1s orbitals of the carbon atoms were excluded from the SAC-CI active space. All single excitation operators were included, and double excitation operators were selected by the perturbation selection method[70,71] using the LevelThree option (note that these singles and doubles were defined as electron processes from the reference closed-shell states). The unlinked terms corresponding to each linked term were calculated using the direct algorithm.[72] The basis sets for the SAC/SAC-CI calculations were D95(d,p) + Dunning's

dx.doi.org/10.1021/jp3051565 | J. Phys. Chem. A 2012, 116, 11833−11845

Table 1. Excitation Characters, Excitation Energies ΔE (eV), Oscillator Strengths f, and Second Moments $\langle r^2 \rangle$ and $\Delta\langle r^2 \rangle$ (au) of the Electronic Ground and Excited States of the Hexatriene Cation Radical

		SAC-CI				exptl[a]
state	character and excitation type	ΔE	f	$\langle r^2 \rangle$	$\Delta\langle r^2 \rangle$[b]	ΔE
X ^2A_u	(ground state)	IE = *7.98*[c]		48.2	0.0	IE = *8.27–8.30*[c,d]
1 ^2B_g	$\pi-\pi_{SOMO}$ - II	2.49	0.235	49.0	0.8	1.93, 1.92,[e] 2.1[f]
2 ^2B_g	$\pi_{SOMO}-\pi^*$ - I	3.13	0.367	49.5	1.3	3.16, 3.27,[e] 3.4[f]
1 ^2A_u	$\pi-\pi_{SOMO}$ - II	3.93	fb[g]	53.6	5.4	
1 ^2A_g	$\sigma-\pi_{SOMO}$ - II	4.41	0.000	47.6	−0.6	
2 ^2A_g	$\sigma-\pi_{SOMO}$ - II	4.87	0.000	51.3	3.1	
1 ^2B_u	$\sigma-\pi_{SOMO}$ - II	4.92	fb[g]	45.3	−2.9	
3 ^2A_g	$\sigma-\pi_{SOMO}$ - II	5.97	0.001	45.6	−2.6	

[a]Reference 8 (in freon mixture) except for the values with notes. [b]Difference in $\langle r^2 \rangle$ between the ground and excited states. The same notation is employed in Tables 2–8. [c]Values in italic represent vertical ionization energies. [d]References 12–14. [e]Reference 14 (in argon). [f]Reference 15 (gas phase). [g]Forbidden. The same notation is employed in Tables 2–8.

diffuse [1s1p] (α = 0.034) for the cation radicals and D95(d,p) + diffuse [3s3p] (α = 0.034, 0.051, and 0.068) for the anion radicals. Although we examined larger basis sets (e.g., triple-ζ, double polarization, and correlation-consistent basis) for several molecules, the results were almost the same as the reported ones.

As mentioned in the Introduction, it is convenient to classify the doublet states into three types (Figure 2). In the present SAC-CI formalism, the type I states of the cation radicals are described by one-electron attachments to the dication SAC state, and those of the anion radicals are described by one-electron attachments to the neutral SAC state. Similarly, the type II states are described as one-electron ionizations from the neutral or dianion SAC state for the cation or anion radicals, respectively. Thus, both type I and type II states are produced from the closed-shell states by single-electron processes. On the other hand, describing the type III excited states of the radicals necessitates ionization or electron attachment followed by single-electron excitation when such states are derived from the closed-shell states. The type III excited states are thus described by two-electron processes from the closed-shell states. Therefore, the SD-R (singles-doubles) method is not accurate enough, and the SAC-CI general-R method[73,74] is required for reliable calculations. However, as described in the Introduction, the type III states usually appear in the higher energy region, which is not the energy region of our interest currently.

3. CATION RADICALS

3.1. Hexatriene and Octatetraene. For the cation radicals of hexatriene and octatetraene, the planar and all-trans structures were the most stable. Furthermore, the energy barriers for the cis–trans isomerizations were calculated to be much higher than the thermal energy at room temperature. Therefore, we consider here all-trans hexatriene and octatetraene cations in C_{2h} symmetry.

We summarize in Table 1 the calculated results for the hexatriene cation radical and compare these with the experimental results.[8,12−15] The summary includes the characters of the electronic ground and excited states, the excitation energies, oscillator strengths, and the second moments. The SOMO for the cation (HOMO for the neutral molecule), SOMO−1, and SOMO−2 are assigned to π orbitals, and the LUMO is assigned to a π^* orbital. Other lower valence occupied orbitals are assigned to σ orbitals. In the upper part of Figure 3, the SAC-CI theoretical spectrum for the hexatriene cation radical is compared with the experimental one observed

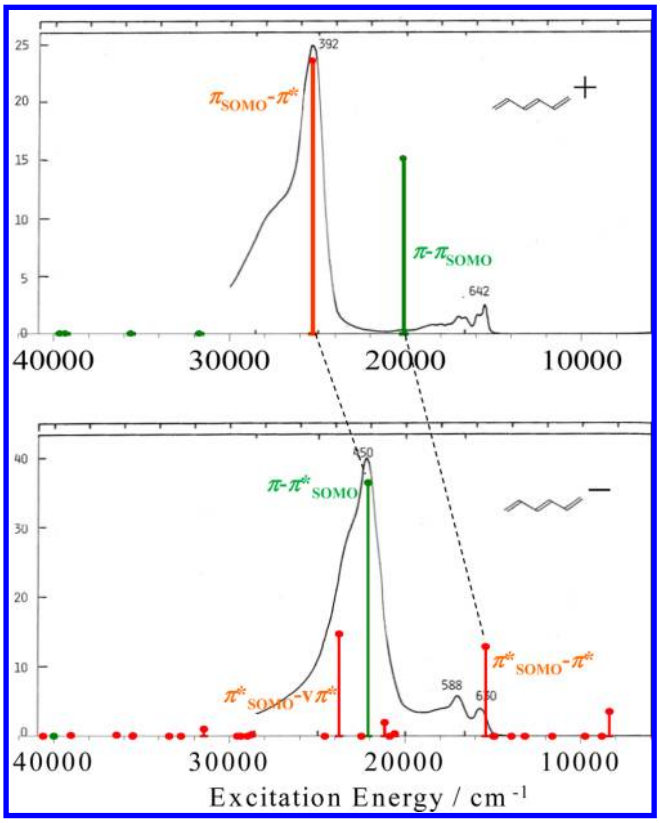

Figure 3. SAC-CI excitation spectra of the hexatriene cation radical (upper) and anion radical (lower) compared with the corresponding experimental ones.[8]

by Shida.[8] The red and green spectral lines represent type I and type II states, respectively. The two bands at ∼16 000 cm^{-1} (∼2.0 eV) and ∼25 000 cm^{-1} (∼3.2 eV) in the excitation spectrum (Figure 3) are assigned to $\pi-\pi_{SOMO}$ (type II) and $\pi_{SOMO}-\pi^*$ (type I) excitations, respectively. Although the energy of the first excited state (1^2B_g) was somewhat overestimated, these assignments are the same as those from the relatively latest experimental[14] and theoretical reports.[14,75] Besides these bands, the forbidden (^2A_u and ^2B_u) and very weak (^2A_g) bands were also calculated in the high energy region. The lowest forbidden band is calculated at 3.93 eV and is assigned to ^2A_u $\pi-\pi_{SOMO}$, whereas the others are assigned to $\sigma-\pi_{SOMO}$. The order of the states does not always agree with that determined from Koopmans' theorem, indicating that the

dx.doi.org/10.1021/jp3051565 | J. Phys. Chem. A 2012, 116, 11833−11845

Table 2. Excitation Characters, Excitation Energies ΔE (eV), Oscillator Strengths f, and Second Moments $\langle r^2 \rangle$ and $\Delta\langle r^2 \rangle$ (au) of the Electronic Ground and Excited States of the Octatetraene Cation Radical

		SAC-CI				exptl[a]
state	character and excitation type	ΔE	f	$\langle r^2 \rangle$	$\Delta\langle r^2 \rangle$	ΔE
X ^2B_g	(ground state)	IE = *7.46*[b]		58.0	0.0	IE = *7.79*[b,c,d]
1 ^2A_u	$\pi-\pi_{SOMO}$ - II	2.20	0.394	56.7	−1.3	1.65, 1.66,[d] 1.66[c,e]
2 ^2A_u	$\pi_{SOMO}-\pi^*$ - I	2.68	0.569	59.8	1.8	2.71, 2.77,[d] 2.94[c,e]
1 ^2B_g	$\pi-\pi_{SOMO}$ - II	3.66	fb	58.0	0.0	
3 ^2A_u	$\pi-\pi_{SOMO}$ - II	4.52	0.003	66.1	8.1	
1 ^2A_g	$\sigma-\pi_{SOMO}$ - II	4.65	fb	56.3	−1.7	
2 ^2B_g	$\pi_{SOMO}-\pi^*$ - I	4.96	fb	61.3	3.3	
1 ^2B_u	$\sigma-\pi_{SOMO}$ - II	5.02	0.000	54.4	−3.6	
2 ^2A_g	$\sigma-\pi_{SOMO}$ - II	5.04	fb	67.1	9.1	
3 ^2A_g	$\sigma-\pi_{SOMO}$ - II	5.67	fb	52.5	−5.5	

[a]Reference 8 (in freon mixture) except for the values with notes. [b]Values in italic represent adiabatic ionization energies. [c]Reference 16 (gas phase). [d]Reference 14 (in argon). [e]Adiabatic excitation energies.

electron correlation effect becomes important for describing the $\sigma-\pi_{SOMO}$ states (Supporting Information). The vertical IE at the neutral ground-state geometry was calculated to be 7.98 eV, which is a bit lower than the experimental values of 8.27,[12] 8.29,[13] and 8.30 eV.[14]

Table 2 shows the calculated results for the octatetraene cation radical, together with the experimental ones.[8,14,16] The four highest occupied MOs including the SOMO are assigned to π orbitals, and the LUMO is assigned to a π^* orbital, similar to the case of the hexatriene cation radical. Other lower valence occupied orbitals are assigned to σ orbitals. The SAC-CI excitation spectrum for the octatetraene cation radical is compared with the experimental one[8] in the upper part of Figure 4. The first peak is assigned to $\pi-\pi_{SOMO}$ (1^2A_u), whose

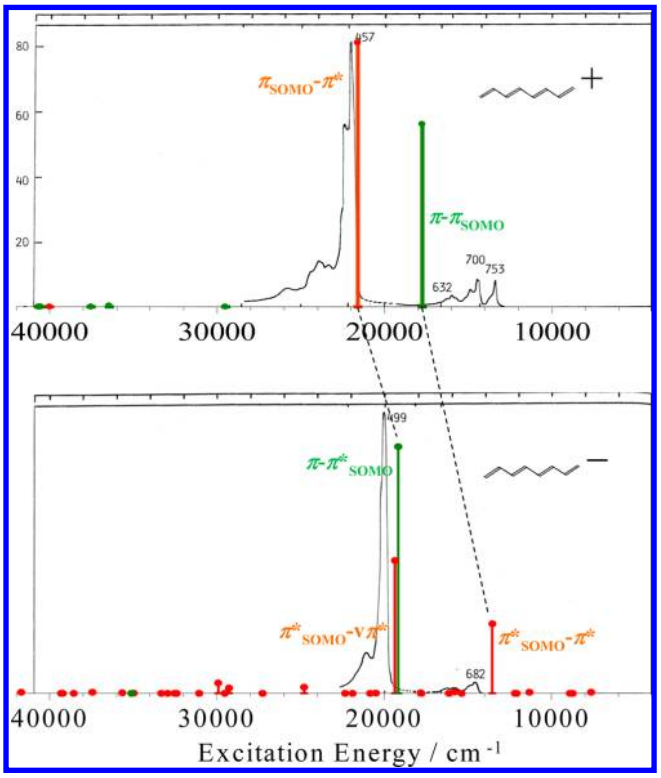

Figure 4. SAC-CI excitation spectra of the octatetraene cation radical (upper) and anion radical (lower) compared with the corresponding experimental ones.[8]

energy was somewhat overestimated. The second strong peak is calculated to be $\pi_{SOMO}-\pi^*$ ($2\ ^2A_u$), and the excitation energy is in good agreement with the experimental results. This result is similar to the previous one for the hexatriene cation. The present assignments are the same as those in the previous experimental[14] and theoretical studies.[14,60] In the higher energy region, several forbidden (^2A_g and ^2B_g) and very weak (^2A_u and ^2B_u) bands were also calculated. They are assigned to $\pi-\pi_{SOMO}$, $\pi-\pi_{SOMO}$, $\sigma-\pi_{SOMO}$, and $\pi_{SOMO}-\pi^*$, in order of increasing energy, whereas the higher ones are assigned to $\sigma-\pi_{SOMO}$. The adiabatic IE of octatetraene was calculated to be 7.46 eV, which is comparable to the experimental value of 7.79 eV.[14,16]

For the hexatriene and octatetraene cation radicals, the first excited states had calculated energies higher than the experimental ones. We improved the basis sets and the perturbation selection thresholds in the SAC-CI calculations, but the results were similar. We think that the deviation from the experimental values can be attributed to the mixing of the first and second excited states that belong to the same symmetry representation. In the present calculations, these two states are calculated separately, and therefore, the mixing of these states may not be well described. This problem can be improved by employing the SAC-CI general-*R* method that can handle many-electron excitations equally well as the ordinary one-electron processes.

3.2. Cyclopentadiene and 1,3-Cyclohexadiene. The cyclopentadiene cation has a planar ring with C_{2v} symmetry at the optimized geometry, whereas the 1,3-cyclohexadiene cation has a nonplanar ring and belongs to the C_2 group. Nevertheless, the *cis*-butadiene skeleton in 1,3-cyclohexadiene is almost planar, and therefore, these two molecules can be regarded as *cis*-butadiene analogs.

The calculated results for the cyclopentadiene and 1,3-cyclohexadiene cation radicals are listed in Tables 3 and 4, respectively, together with the experimental results.[8,17,18] The corresponding theoretical (this work) and experimental[8] excitation spectra are shown in Figures 5 and 6 (upper illustrations), respectively, together with the calculated results for *cis*-butadiene as a reference (lower illustrations). For both molecules, only the HOMOs (SOMOs in fact) and next-HOMOs are assigned to π orbitals, and other valence occupied orbitals are assigned to σ orbitals. The LUMOs of these cations are assigned as having π^* character. For both cations, the first excited states are assigned to $\pi-\pi_{SOMO}$ (type II) and the second ones to $\pi_{SOMO}-\pi^*$ (type I). Except for the second excited

dx.doi.org/10.1021/jp3051565 | J. Phys. Chem. A 2012, 116, 11833−11845

Table 3. Excitation Characters, Excitation Energies ΔE (eV), Oscillator Strengths f, and Second Moments $\langle r^2 \rangle$ and $\Delta\langle r^2 \rangle$ (au) of the Electronic Ground and Excited States of the Cyclopentadiene Cation Radical

		SAC-CI				exptl[a]
state	character and excitation type	ΔE	f	$\langle r^2 \rangle$	$\Delta\langle r^2 \rangle$	ΔE
X $^2A_2$	(ground state)	IE = *8.38*[b]		48.7	0.0	IE = *8.44*[b,c]
1 $^2B_1$	$\pi-\pi_{SOMO}$ - II	2.41	0.048	48.3	−0.4	2.23
2 $^2B_1$	$\pi_{SOMO}-\pi^*$ - I	3.68	0.053	48.9	0.2	3.37
1 $^2B_2$	$\sigma-\pi_{SOMO}$ - II	4.02	0.000	47.1	−1.6	
1 $^2A_1$	$\sigma-\pi_{SOMO}$ - II	4.46	fb	47.3	−1.4	
2 $^2A_1$	$\sigma-\pi_{SOMO}$ - II	4.52	fb	46.7	−2.0	
2 $^2B_2$	$\sigma-\pi_{SOMO}$ - II	4.91	0.000	46.3	−2.4	

[a]Reference 8 (in freon mixture) except for the values with notes. [b]Values in italic represent vertical ionization energies. [c]Reference 17.

Table 4. Excitation Characters, Excitation Energies ΔE (eV), Oscillator Strengths f, and Second Moments $\langle r^2 \rangle$ and $\Delta\langle r^2 \rangle$ (au) of the Electronic Ground and Excited States of the 1,3-Cyclohexadiene Cation Radical

		SAC-CI				exptl[a]
state	character and excitation type	ΔE	f	$\langle r^2 \rangle$	$\Delta\langle r^2 \rangle$	ΔE
X ^2A	(ground state)	IE = *8.02*[b]		59.3	0.0	IE = *8.25*[b,c]
1 ^2B	$\pi-\pi_{SOMO}$ - II	3.05	0.097	60.1	0.8	2.62
2 ^2B	$\pi_{SOMO}-\pi^*$ - I	3.21	0.083	59.7	0.4	3.20
1 ^2A	$\sigma-\pi_{SOMO}$ - II	3.55	0.001	57.9	−1.4	
3 ^2B	$\sigma-\pi_{SOMO}$ - II	3.77	0.002	58.1	−1.2	
2 ^2A	$\sigma-\pi_{SOMO}$ - II	5.00	0.083	59.0	−0.3	

[a]Reference 8 (in freon mixture) except for the values with notes. [b]Values in italic represent vertical ionization energies. [c]Reference 18.

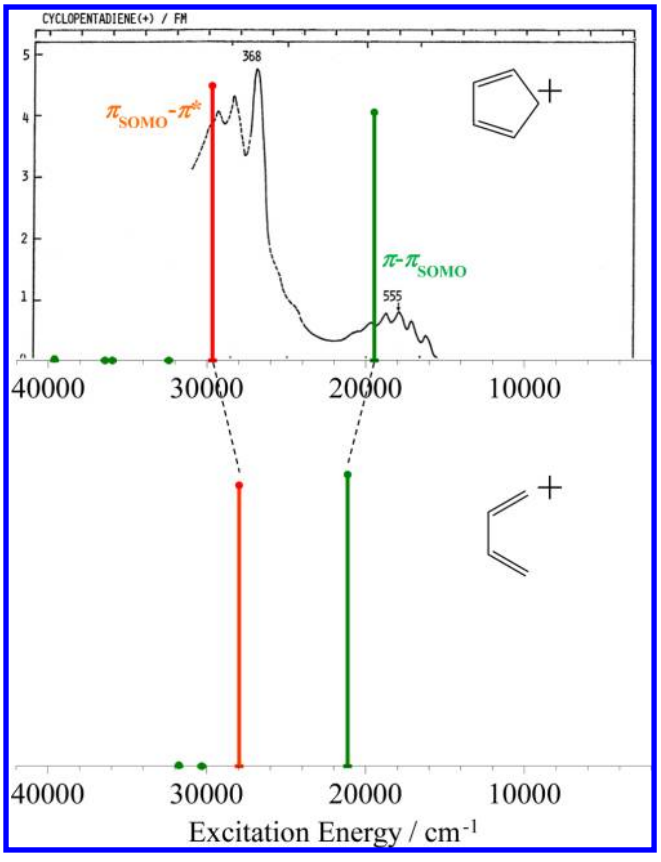

Figure 5. SAC-CI excitation spectrum of the cyclopentadiene cation radical compared with the experimental one[8] (upper) and the calculated spectrum of *cis*-butadiene for reference (lower).

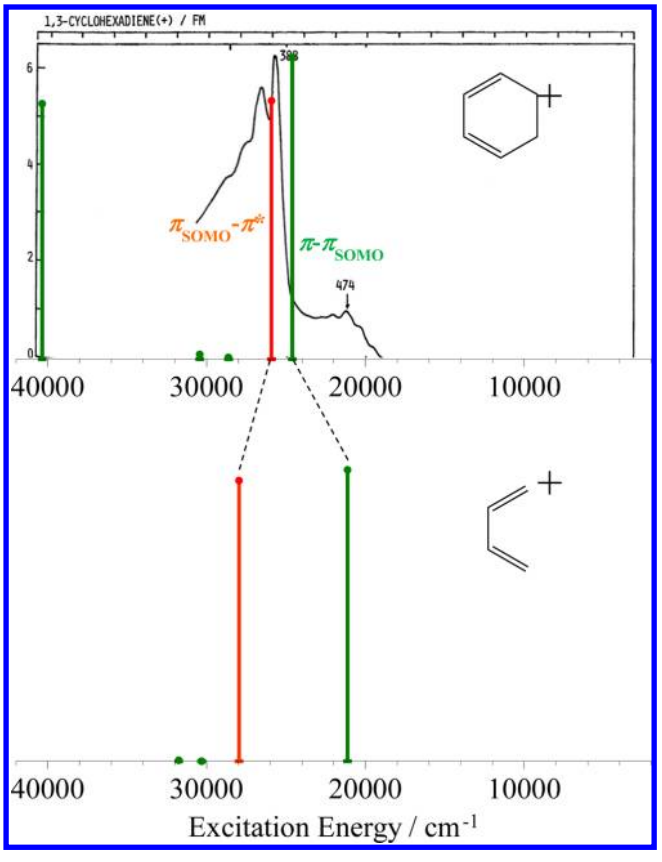

Figure 6. SAC-CI excitation spectrum of the 1,3-cyclohexadiene cation radical compared with the experimental one[8] (upper) and the calculated spectrum of *cis*-butadiene for reference (lower).

states, all the states are categorized as type II excitations, and the higher states are described by $\sigma-\pi_{SOMO}$ transitions. For 1,3-cyclohexadiene, both calculated states might correspond to the second band at ~26 000 cm^{-1} (~3.2 eV) in Figure 6. However, we assigned the calculated state at 3.05 eV to the first band at ~21 000 cm^{-1} (~2.6 eV) in the experiment, because no

dx.doi.org/10.1021/jp3051565 | J. Phys. Chem. A 2012, 116, 11833−11845

Table 5. Excitation Characters, Excitation Energies ΔE (eV), Oscillator Strengths f, and Second Moments $\langle r^2 \rangle$ and $\Delta\langle r^2 \rangle$ (au) of the Electronic Ground and Excited States of the Naphthalene Cation Radical

		SAC-CI				exptl[a]
state	character and excitation type	ΔE	f	$\langle r^2 \rangle$	$\Delta\langle r^2 \rangle$	ΔE
X ^2A_u	(ground state)	IE = *7.80*[b]		92.6	0.0	IE = *8.144*,[b,c] *8.12*[b,d]
1 $^2B_{3u}$	$\pi-\pi_{SOMO}$ - II	0.76	fb	91.9	−0.7	0.73[e]
1 $^2B_{2g}$	$\pi-\pi_{SOMO}$ - II	2.00	0.139	94.2	1.6	1.80, 1.76, 1.84[f,g,h]
1 $^2B_{1g}$	$\pi-\pi_{SOMO}$ - II	3.15	0.106	91.1	−1.5	2.65, 2.56, 2.69;[f] 2.72[g,h]
1 ^2A_g	$\sigma-\pi_{SOMO}$ - II	3.40	fb	91.1	−1.5	
1 $^2B_{3g}$	$\sigma-\pi_{SOMO}$ - II	3.41	0.000	89.5	−3.1	
2 $^2B_{1g}$	$\pi_{SOMO}-\pi^*$ - I	3.45	0.010	92.4	−0.2	3.20, 3.14, 3.25;[f] 3.29[g]
1 $^2B_{2u}$	$\sigma-\pi_{SOMO}$ - II	4.59	fb	88.9	−3.7	
2 $^2B_{3u}$	$\pi-\pi_{SOMO}$ - II	4.85	fb	94.6	2.0	
2 $^2B_{2g}$	$\pi_{SOMO}-\pi^*$ - I[i]	5.02	0.116	94.0	1.4	4.03, 3.99, 4.02;[f] ∼4.07[g]

[a]Reference 8 (in freon mixture or *s*-BuCl) except for the values with notes. [b]Values in italic represent vertical ionization energies. [c]Reference 19. [d]Reference 20. [e]Reference 21 (photoelectron spectrum at the neutral geometry). [f]Reference 21 (in argon). [g]Reference 22 (gas phase). [h]Reference 23 (in argon). [i]To be accurate, $0.90(\pi_{SOMO}-\pi^*) + 0.37(\pi-\pi_{SOMO})$.

electronic states were calculated below this state. The energy gap between the lowest calculated and experimental bands for the cyclohexadiene cation is expected to be due to interaction between the first and second states having the same symmetry (B). The vertical IEs of cyclopentadiene and 1,3-cyclohexadiene were calculated to be 8.38 and 8.02 eV, respectively. These are in fairly good agreement with the corresponding experimental values of 8.44[17] and 8.25 eV.[18]

On the other hand, two intense excited states were calculated for the *cis*-butadiene cation radical. Their energy positions and characters were very similar to those for the cyclopentadiene and 1,3-cyclohexadiene cation radicals. The similarity among these three cations can be attributed to the presence of a common, almost planar butadiene skeleton in the cycloalkanes.

3.3. Naphthalene. The naphthalene cation is planar at the optimized geometry and belongs to the D_{2h} group. In this study, we define the molecular axes as in Figure 1, namely the x-axis is perpendicular to the molecular plane, and the y- and z-axes are parallel to the long and short axes on the plane, respectively. One should be careful when comparing our data to those in the literature because another definition is often employed (e.g., the z-axis being perpendicular to the molecular plane).

Table 5 shows the SAC-CI results of the electronic ground and excited states for the naphthalene cation radical, along with the experimental results.[8,19−23] The corresponding calculated excitation spectrum is compared with the experimental one[8] in the upper part of Figure 7. The characters of the occupied orbitals from the SOMO (in order of decreasing orbital energy) are π_{SOMO}, π, π, π, σ, σ, π, and σ. The LUMO and LUMO+1 are assigned to π^* orbitals.

According to our calculations, the first excited state is a forbidden $\pi-\pi_{SOMO}$ state ($1\ ^2B_{3u}$, type II). This reasonably corresponds to the first ionization peak, 0.73 eV above the cation ground state, in the photoelectron spectrum at the neutral geometry.[21] Four intense peaks were calculated (2.00 ($1\ ^2B_{2g}$), 3.15 ($1\ ^2B_{1g}$), 3.45 ($2\ ^2B_{1g}$), and 5.02 eV ($2\ ^2B_{2g}$)) and assigned to $\pi-\pi_{SOMO}$ (type II), $\pi-\pi_{SOMO}$ (type II), $\pi_{SOMO}-\pi^*$ (type I), and $\pi_{SOMO}-\pi^*$ (type I), respectively. On the other hand, in the experimental spectra, four states were observed (∼1.8, ∼2.7, ∼3.2, and ∼4.0 eV). The lowest intense peak (∼1.8 eV) is naturally assigned to the type II $\pi-\pi_{SOMO}$ transition. The assignments of the second and third peaks are provided in Figure 7, judging from the experiments on the

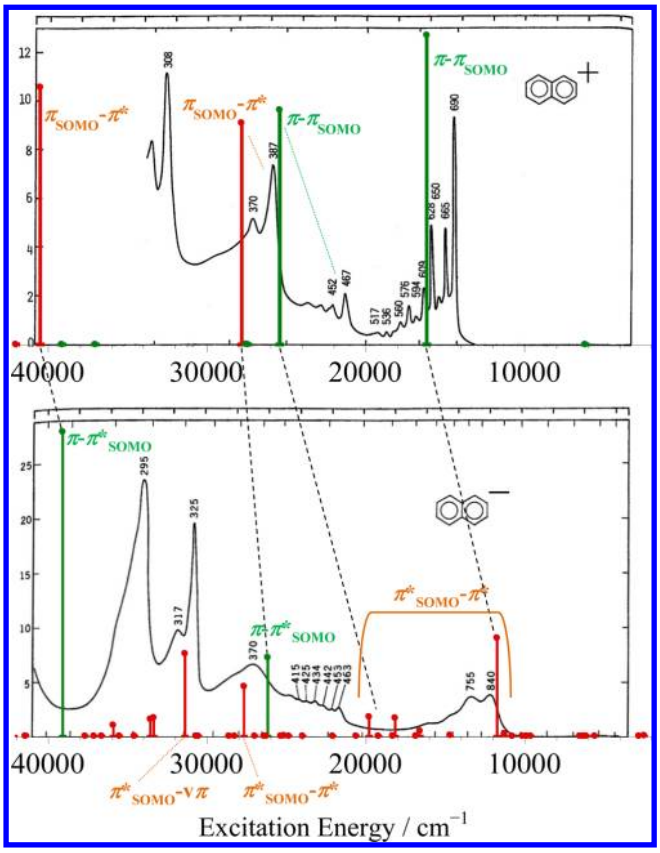

Figure 7. SAC-CI excitation spectra of the naphthalene cation radical (upper) and anion radical (lower) compared with the corresponding experimental ones[8] for band assignments.

transition direction of these bands. These assignments are in accordance with the previous experimental[21] and theoretical reports.[21,76−79] For the highest intense state at 5.02 eV in our calculations, we assigned it to the experimental band at ∼4.0 eV. However, this assignment is tentative because several experiments reported the fifth state at ∼4.5 eV.[21,27,28] According to CASPT2 calculations by Bally et al.,[21] the fourth state (∼4.0 eV) had substantial $\pi_{SOMO}-\pi^*$ character (type I) and the fifth (∼4.5 eV) was dominantly described by $\pi-\pi^*$ excitations beyond the SOMO (type III). On the other hand, recent TDDFT calculations by Malloci et al.[79] suggested that

dx.doi.org/10.1021/jp3051565 | J. Phys. Chem. A 2012, 116, 11833−11845

Table 6. Excitation Characters, Excitation Energies ΔE (eV), Oscillator Strengths f, and Second Moments $\langle r^2 \rangle$ and $\Delta\langle r^2 \rangle$ (au) of the Electronic Ground and Excited States of the Hexatriene Anion Radical

	SAC-CI					exptl[a]
state	character and excitation type[b]	ΔE	f	$\langle r^2 \rangle$	$\Delta\langle r^2 \rangle$	ΔE
X ^2B_g	(ground state)	EA = *−0.43*[c]		127.9	0.0	
1 ^2A_g	$\pi^*_{SOMO}-\sigma^*$ - I	0.49	fb	191.8	63.9	
1 ^2B_u	$\pi^*_{SOMO}-\sigma^*$ - I	0.66	0.010	222.1	94.2	
2 ^2B_u	$\pi^*_{SOMO}-\sigma^*$ - I	0.72	0.000	172.5	44.6	
1 ^2A_u	$\pi^*_{SOMO}-\pi^*$ - I	1.04	0.052	183.5	55.6	
2 ^2A_g	$\pi^*_{SOMO}-\sigma^*$ - I	1.09	fb	216.1	88.2	
3 ^2A_g	$\pi^*_{SOMO}-\sigma^*$ - I	1.21	fb	209.2	81.3	
1 ^2B_g	$\pi^*_{SOMO}-\pi^*$ - I	1.44	fb	208.4	80.5	
2 ^2B_g	$\pi^*_{SOMO}-\pi^*$ - I	1.63	fb	173.6	45.7	
3 ^2B_u	$\pi^*_{SOMO}-\sigma^*$ - I	1.73	0.000	220.4	92.5	
4 ^2B_u	$\pi^*_{SOMO}-\sigma^*$ - I	1.85	0.000	210.2	82.3	
4 ^2A_g	$\pi^*_{SOMO}-v\sigma^*$ - I	1.85	fb	166.0	38.1	
2 ^2A_u	$\pi^*_{SOMO}-\pi^*$ - I	1.91	0.186	191.6	63.7	1.97
3 ^2A_u	$\pi^*_{SOMO}-\pi^*$ - I	2.55	0.005	183.4	55.5	
5 ^2A_g	$\pi^*_{SOMO}-\sigma^*$ - I	2.59	fb	217.0	89.1	
5 ^2B_u	$\pi^*_{SOMO}-\sigma^*$ - I	2.62	0.029	186.1	58.2	
4 ^2A_u	$\pi-\pi^*_{SOMO}$ - II	2.74	0.527	134.6	6.7	2.76
6 ^2A_g	$\pi^*_{SOMO}-\sigma^*$ - I	2.79	fb	204.4	76.5	
5 ^2A_u	$\pi^*_{SOMO}-v\pi^*$ - I	2.95	0.212	163.6	35.7	
3 ^2B_g	$\pi^*_{SOMO}-\pi^*$ - I	3.05	fb	208.1	80.2	
6 ^2B_u	$\pi^*_{SOMO}-\sigma^*$ - I	3.56	0.004	183.8	55.9	
4 ^2B_g	$\pi^*_{SOMO}-v\pi^*$ - I	3.60	fb	144.1	16.2	
7 ^2A_g	$\pi^*_{SOMO}-\sigma^*$ - I	3.64	fb	187.9	60.0	
7 ^2B_u	$\pi^*_{SOMO}-\sigma^*$ - I	3.67	0.000	185.6	57.7	
8 ^2B_u	$\pi^*_{SOMO}-\sigma^*$ - I	3.90	0.015	201.9	74.0	
8 ^2A_g	$\pi^*_{SOMO}-\sigma^*$ - I	4.06	fb	191.2	63.3	
9 ^2A_g	$\pi^*_{SOMO}-\sigma^*$ - I	4.14	fb	179.1	51.2	
9 ^2B_u	$\pi^*_{SOMO}-\sigma^*$ - I	4.40	0.001	192.7	64.8	
10 ^2A_g	$\pi^*_{SOMO}-\sigma^*$ - I	4.40	fb	185.1	57.2	
6 ^2A_u	$\pi^*_{SOMO}-v\pi^*$ - I	4.52	0.003	159.5	31.6	
10 ^2B_u	$\pi^*_{SOMO}-\sigma^*$ - I	4.84	0.002	175.9	48.0	
5 ^2B_g	$\pi-\pi^*_{SOMO}$ - II	4.96	fb	139.6	11.7	
6 ^2B_g	$\pi^*_{SOMO}-\pi^*$ - I	5.03	fb	182.4	54.5	

[a]Reference 8 (in MTHF). [b]Simple "π^*" and "σ^*" denote diffuse-mixed π^* and σ^* characters, respectively, whereas "vπ^*" and "vσ^*" mean valence π^* and valence σ^*, respectively. The same notation is employed in Tables 7 and 8. [c]Value in italic represents the vertical electron affinity.

the fourth and fifth states were assigned to type III $\pi-\pi^*$ and type I $\pi_{SOMO}-\pi^*$, respectively. The 2 $^2B_{2g}$ state in our calculations includes a considerable contribution of a two-electron process from the SAC configuration, which reduces the accuracy of the SD-*R* method. To examine which interpretation is correct, a more accurate calculation is required using the general-*R* method that can treat type III excitations explicitly.

The vertical IE at the neutral geometry was calculated to be 7.80 eV and is in agreement with the experimental values of 8.144[19] and 8.12 eV.[20]

4. ANION RADICALS

Before we report the result of each anion radical, it may be important to recognize the relationship between the above-mentioned excitation types and the two resonance mechanisms, the shape and Feshbach resonances.[65,80−83] All the electron-attached excited states of the target molecules lie above their electron detachment thresholds, namely above the energies of the neutral molecules. Therefore, none of the excited states of the hexatriene, octatetraene, or naphthalene anion radicals are bound states; rather, they are metastable and can be observed only as resonance states. In this study, type I and II excitations of the anions correspond to the shape and Feshbach resonances, respectively. Detachment from each type I excited state gives the neutral ground state, indicating that type I excitations must induce shape resonances, as seen in Figure 2. On the other hand, detachments from type II states produce neutral excited states, not ground states, and therefore, Feshbach resonances would occur. (Strictly speaking, shape resonance would occur if the anion excited state has a higher energy than the electron-detached excited state. In this study, the neutral excited state formed from each anion excited state is always located above the corresponding anion state.)

In general, most unoccupied orbitals of anions have diffuse characters, and it is not easy to give assignments to them. We determined the assignments of the states described by such orbitals, judging from the values of the second moments, and more precisely, the difference in the second moment between the ground and excited states of each molecule.[83] For simplicity, we will refer to the diffuse-mixed π^* and σ^* characters of the anion states as "π^*" and "σ^*," respectively. On the other hand, valence π^* and σ^* characters (with small

second moments) will be specifically represented as "vπ*" and "vσ*," respectively.

4.1. Hexatriene and Octatetraene. Both these anions were planar and all-trans at the most stable geometries. The energy barriers for the cis−trans isomerizations were much higher than the thermal energy. Therefore, we consider only the all-trans hexatriene and octatetraene anions in C_{2h} symmetry group.

The calculated results for the hexatriene anion radical are summarized in Table 6. The table shows the characters, excitation energies, oscillator strengths, and second moments of the electronic states, together with the experimental results.[8] The SOMO for the anion (LUMO for the neutral molecule) is assigned to valence π*. Similar to the case of the hexatriene cation, the SOMO−1 (HOMO for the neutral molecule) and SOMO−2 are assigned to valence π.

The SAC-CI theoretical (this work) and experimental[8] spectra for the hexatriene anion radical are shown in the lower part of Figure 3. The calculated spectrum shows fairly good agreement with the experimental one. The first band at ∼16 000 cm^{-1} (∼2.0 eV) in the experiment corresponds to the $\pi^*_{SOMO}-\pi^*$ shape resonance state (type I) in our calculations. The second band at ∼22 000 cm^{-1} (∼2.7 eV) is assigned to the $\pi-\pi^*_{SOMO}$ Feshbach resonance state (type II). In addition, an intense state due to $\pi^*_{SOMO}-v\pi^*$ (type I) was found at 2.95 eV in our calculations and can be assigned to the left shoulder of the second band in the experiment. These three intense states belong to ^2A_u. Our calculations predict valence excited states with no or very small intensities at 3.60, 4.52, and 4.96 eV, and they are assigned to $\pi^*_{SOMO}-v\pi^*$ (^2B_g), $\pi^*_{SOMO}-v\pi^*$ (^2A_u), and $\pi-\pi^*_{SOMO}$ (^2B_g), respectively. Besides the above valence states, many diffuse states were also calculated. Their second moments (170−230 au) were much larger than that of the ground state (127.9 au), and the energy positions varied with respect to the basis set extension. Therefore, we think that these diffuse states are insignificant in this study. The adiabatic EA at the neutral ground-state geometry was calculated to be −0.43 eV. The experimental value of the EA for hexatriene is unknown. Burrow and Jordan suggested a positive EA[29] on the basis of the pairing theorem,[35,40−46] whereas Staley and Strnad estimated negative values (−0.2 to −0.3 eV)[40] using ab initio calculations. Our results support the latter estimates.

The experimental spectrum in Figure 3 was measured in 2-methyltetrahydrofuran (MTHF) matrices,[8] not in the gas phase. We performed the SAC-CI calculations for the hexatriene anion with tetrahydrofuran (THF) molecules to estimate this solvent effect (the interaction between the hexatriene molecule and the methyl group of MTHF was very weak in preliminary calculations, and we ignored the methyl groups). The examined geometry, which was optimized by UB3LYP/D95+(d,p) with the C_i-symmetry constraint, is shown in Figure 8. The negative charge was well localized on the hexatriene molecule, and the two THF molecules were almost neutral. The hexatriene−THF binding energy was 4.8 kcal/mol, and the hexatriene remained planar in this system. Thus, the interaction between the hexatriene anion and (M)THF is expected to be relatively weak. The SAC-CI calculations were performed on the hexatriene anion sandwiched between point charges expressing the two THF molecules (Mulliken and natural population analyses with the B3LYP density functional). The results showed that THF had limited influence on the spectral trends for both population analyses, indicating that the solvent effect of MTHF is small.

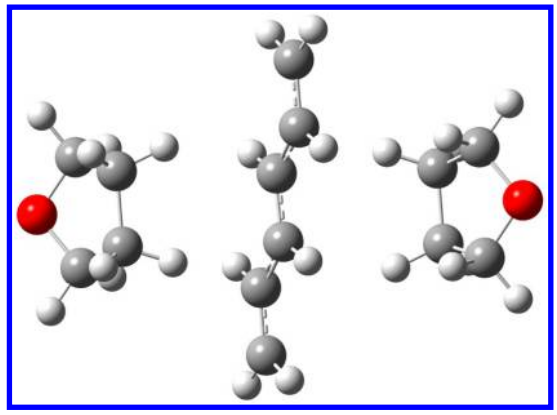

Figure 8. Optimized geometry of the hexatriene anion with two THF molecules.

Table 7 shows the calculated results for the electronic ground and excited states of the octatetraene anion radical, accompanied by the corresponding experimental results.[8,30] The adiabatic EA of octatetraene was calculated to be 0.043 eV, indicating that the ground state of the octatetraene anion is slightly more stable than the neutral ground state. Although the experimental EA value is unknown, Allan et al. suggested a positive EA,[30] which was supported by estimations based on the calculations of Staley and Strnad (+0.04 to +0.13 eV).[40] Our results also support these suggestions, and it is expected that the crossover from negative to positive EAs in the linear polyenes occurs between hexatriene and octatetraene. The SOMO for the anion (LUMO for the neutral molecule) is assigned to valence π*, and the SOMO−1 (HOMO for the neutral molecule) and SOMO−2 are assigned to valence π.

The excitation spectra for the octatetraene anion radical obtained theoretically (this work) and experimentally[8] are shown in the lower part of Figure 4. The calculated spectrum of the octatetraene anion agrees well with the experimental one. The first band at ∼15 000 cm^{-1} (∼1.8 eV) in the experiment is assigned to the $\pi^*_{SOMO}-\pi^*$ shape resonance state (type I), and the second band at ∼20 000 cm^{-1} (∼2.5 eV) is assigned to the $\pi-\pi^*_{SOMO}$ Feshbach resonance state (type II). An additional intense state of $\pi^*_{SOMO}-v\pi^*$ (type I) was calculated at 2.40 eV and can be assigned to the left shoulder of the second band in the experiment. These trends are very similar to those of the hexatriene anion, but in this case, these three intense states belong to ^2B_g. Our calculations predict valence excited states with no or very small intensities at 1.96, 2.21, 4.02, 4.03, 4.35, and 4.86 eV, which are assigned to $\pi^*_{SOMO}-v\pi^*$ (^2B_g), $\pi^*_{SOMO}-v\sigma^*$ (^2A_g), $\pi^*_{SOMO}-v\sigma^*$ (^2B_u), $\pi^*_{SOMO}-v\pi^*$ (^2B_g), $\pi-\pi^*_{SOMO}$ (^2A_u), and $\pi^*_{SOMO}-v\pi^*$ (^2A_u), respectively. Allan et al. reported anion excited states at 1.50, 2.52, and 4.16 eV above the neutral ground state,[30] which correspond to 1.54, 2.56, and 4.20 eV, respectively, above the anion ground state assuming our calculated EA, 0.04 eV. The states at 1.54 and 4.20 eV are naturally assigned to 1 ^2B_g and 7 ^2B_g in our calculations. These assignments are in accordance with those by Allan et al. On the other hand, the state at 2.56 eV was assigned to the ^2A_u state in ref 30, whereas it can be assigned to either 4 ^2B_g or 3 ^2A_u in our calculations. The energies of these two states are similar, so we cannot give definite assignments at the present stage. It is inconsistent to assign the state at 2.56 eV to 3 ^2B_g because the 3 ^2B_g state is described by the type II excitation, which is difficult to observe by electron transmission spectroscopy.

dx.doi.org/10.1021/jp3051565 | J. Phys. Chem. A 2012, 116, 11833−11845

Table 7. Excitation Characters, Excitation Energies ΔE (eV), Oscillator Strengths f, and Second Moments $\langle r^2 \rangle$ and $\Delta\langle r^2 \rangle$ (au) of the Electronic Ground and Excited States of the Octatetraene Anion Radical

		SAC-CI				exptl[a]
state	character and excitation type	ΔE	f	$\langle r^2 \rangle$	$\Delta\langle r^2 \rangle$	ΔE
X ^2A_u	(ground state)	EA = *0.043*[b]		170.5	0.0	
1 ^2A_g	$\pi^*_{SOMO}-\sigma^*$ - I	0.95	0.004	236.0	65.5	
1 ^2B_u	$\pi^*_{SOMO}-\sigma^*$ - I	1.08	fb	220.9	50.4	
2 ^2B_u	$\pi^*_{SOMO}-\sigma^*$ - I	1.10	fb	270.4	99.9	
2 ^2A_g	$\pi^*_{SOMO}-\sigma^*$ - I	1.41	0.003	276.3	105.8	
1 ^2A_u	$\pi^*_{SOMO}-\pi^*$ - I	1.50	fb	220.9	50.4	
3 ^2A_g	$\pi^*_{SOMO}-\sigma^*$ - I	1.51	0.000	254.1	83.6	
1 ^2B_g	$\pi^*_{SOMO}-\pi^*$ - I	1.68	0.198	259.5	89.0	1.82, 1.54[c]
3 ^2B_u	$\pi^*_{SOMO}-\sigma^*$ - I	1.91	fb	275.3	104.8	
2 ^2B_g	$\pi^*_{SOMO}-v\pi^*$ - I	1.96	0.004	206.2	35.7	
4 ^2B_u	$\pi^*_{SOMO}-\sigma^*$ - I	2.00	fb	277.1	106.6	
2 ^2A_u	$\pi^*_{SOMO}-\pi^*$ - I	2.21	fb	266.5	96.0	
4 ^2A_g	$\pi^*_{SOMO}-v\sigma^*$ - I	2.21	0.002	205.8	35.3	
3 ^2B_g	$\pi-\pi^*_{SOMO}$ - II	2.38	0.703	174.0	3.5	2.48
4 ^2B_g	$\pi^*_{SOMO}-v\pi^*$ - I	2.40	0.379	186.9	16.4	2.56?[c,d]
5 ^2A_g	$\pi^*_{SOMO}-\sigma^*$ - I	2.54	0.001	278.1	107.6	
3 ^2A_u	$\pi^*_{SOMO}-\pi^*$ - I	2.59	fb	229.9	59.4	2.56?[c,d]
6 ^2A_g	$\pi^*_{SOMO}-\sigma^*$ - I	2.72	0.000	260.2	89.7	
5 ^2B_u	$\pi^*_{SOMO}-\sigma^*$ - I	2.77	fd	230.5	60.0	
5 ^2B_g	$\pi^*_{SOMO}-\pi^*$ - I	3.08	0.018	263.0	92.5	
6 ^2B_u	$\pi^*_{SOMO}-\sigma^*$ - I	3.38	fd	266.7	96.2	
7 ^2A_g	$\pi^*_{SOMO}-\sigma^*$ - I	3.63	0.015	238.8	68.3	
7 ^2B_u	$\pi^*_{SOMO}-\sigma^*$ - I	3.66	fd	250.8	80.3	
6 ^2B_g	$\pi^*_{SOMO}-\pi^*$ - I	3.71	0.030	226.7	56.2	
4 ^2A_u	$\pi^*_{SOMO}-\pi^*$ - I	3.85	fb	215.7	45.2	
8 ^2B_u	$\pi^*_{SOMO}-v\sigma^*$ - I	4.02	fb	205.3	34.8	
7 ^2B_g	$\pi^*_{SOMO}-v\pi^*$ - I	4.03	fb	195.5	25.0	4.20[c]
8 ^2A_g	$\pi^*_{SOMO}-\sigma^*$ - I	4.03	0.000	242.3	71.8	
5 ^2A_u	$\pi^*_{SOMO}-\pi^*$ - I	4.08	fb	234.4	63.9	
9 ^2B_u	$\pi^*_{SOMO}-\sigma^*$ - I	4.13	fb	266.8	96.3	
9 ^2A_g	$\pi^*_{SOMO}-\sigma^*$ - I	4.34	0.001	222.5	52.0	
6 ^2A_u	$\pi-\pi^*_{SOMO}$ - II[e]	4.35	fb	201.7	31.2	
10 ^2A_g	$\pi^*_{SOMO}-\sigma^*$ - I	4.42	0.002	262.1	91.6	
11 ^2A_g	$\pi^*_{SOMO}-\sigma^*$ - I	4.64	0.004	241.3	70.8	
10 ^2B_u	$\pi^*_{SOMO}-\sigma^*$ - I	4.78	fb	252.6	82.1	
7 ^2A_u	$\pi^*_{SOMO}-v\pi^*$ - I	4.86	fb	199.1	28.6	
11 ^2B_u	$\pi^*_{SOMO}-\sigma^*$ - I	4.88	fb	237.3	66.8	

[a]Reference 8 (in MTHF) except for the values with notes. [b]Value in italic represents the adiabatic electron affinity. [c]Reference 30 (gas phase) assuming our calculated EA, 0.04 eV. [d]The state observed at 2.56 eV in ref 30 can be assigned to either 4 ^2B_g or 3 ^2A_u. [e]To be accurate, $0.66(\pi-\pi^*_{SOMO}) + 0.82(\pi^*_{SOMO}-\pi^*)$.

4.2. Naphthalene. Naphthalene maintains planar D_{2h} symmetry even when it is anionized. The definition for the molecular axes is the same as that for the cation, namely the x-axis is perpendicular to the molecular plane, and the y- and z-axes are parallel to the long and short axes on the plane, respectively.

The calculated results for the naphthalene anion radical are summarized in Table 8, along with the corresponding experimental results.[8,31−36] The adiabatic EA of naphthalene was calculated to be −0.33 eV, which is comparable to the experimental values of −0.2[31,32] and −0.18 eV.[33] Because naphthalene has a negative EA, all states of its anion radical can exist only as resonance states. The SOMO for the anion (LUMO for the neutral molecule) is assigned to valence π^*, and the SOMO−1 (HOMO for the neutral molecule) and SOMO−2 have valence π characters.

The lower part of Figure 7 shows the SAC-CI theoretical and experimental[8] excitation spectra for the naphthalene anion radical. The first band at ∼12 000 cm^{-1} (∼1.5 eV) in the experiment is assigned to a shape resonance state ($^2B_{3u}$) owing to the transitions from π^*_{SOMO} to π^*. The second band at ∼22 000 cm^{-1} (∼2.7 eV), probably with vibrational structures, is expected to consist of $\pi^*_{SOMO}-\pi^*$ shape resonance states ($^2B_{3u}$). The third band at ∼27 000 cm^{-1} (∼3.4 eV) is assigned to $\pi-\pi^*_{SOMO}$ (^2A_u), which is the lowest Feshbach resonance state in this system. Our calculations predict a moderately intense state because of $\pi^*_{SOMO}-\pi^*$ shape resonance (^2A_u) at 3.43 eV, which is expected to form the left shoulder of the third band in the experiment. The fourth band having a large intensity at ∼31 000 cm^{-1} (∼3.8 eV) is assigned to a $\pi^*_{SOMO}-v\pi^*$ shape resonance state (^2A_u). Finally, the fifth band at ∼34 000 cm^{-1} (∼4.2 eV) is assigned to the second Feshbach resonance state ($^2B_{3u}$) with a $\pi-\pi^*_{SOMO}$ character. This

dx.doi.org/10.1021/jp3051565 | J. Phys. Chem. A 2012, 116, 11833−11845

Table 8. Excitation Characters, Excitation Energies ΔE (eV), Oscillator Strengths f, and Second Moments $\langle r^2 \rangle$ and $\Delta\langle r^2 \rangle$ (au) of the Electronic Ground and Excited States of the Naphthalene Anion Radical

		SAC-CI				exptl[a]
state	character and excitation type	ΔE	f	$\langle r^2 \rangle$	$\Delta\langle r^2 \rangle$	ΔE
X $^2B_{1g}$	(ground state)	EA = −0.33[b]		163.9	0.0	EA = *−0.2*,[b,c] *−0.18*[b,d]
1 ^2A_g	$\pi^*_{SOMO}-\sigma^*$ - I	0.09	fb	236.1	72.2	
1 $^2B_{2u}$	$\pi^*_{SOMO}-\sigma^*$ - I	0.31	0.001	255.5	91.6	
1 $^2B_{1u}$	$\pi^*_{SOMO}-\sigma^*$ - I	0.35	fb	237.9	74.0	
1 $^2B_{3u}$	$\pi^*_{SOMO}-\pi^*$ - I	0.69	0.000	221.8	57.9	
2 ^2A_g	$\pi^*_{SOMO}-\sigma^*$ - I	0.76	fb	256.4	92.5	
1 $^2B_{3g}$	$\pi^*_{SOMO}-\sigma^*$ - I	0.78	fb	259.3	95.4	
1 $^2B_{2g}$	$\pi^*_{SOMO}-v\pi^*$ - I	0.81	fb	178.6	14.7	0.97,[e] 0.71[f]
1 $^2B_{1g}$	$\pi^*_{SOMO}-\pi^*$ - I	1.19	fb	244.3	80.4	
3 ^2A_g	$\pi^*_{SOMO}-\sigma^*$ - I	1.22	fb	210.5	46.6	
2 $^2B_{2g}$	$\pi^*_{SOMO}-\pi^*$ - I	1.25	fb	225.6	61.7	
2 $^2B_{1u}$	$\pi^*_{SOMO}-\sigma^*$ - I	1.33	fb	267.6	103.7	
2 $^2B_{2u}$	$\pi^*_{SOMO}-\sigma^*$ - I	1.39	0.003	259.3	95.4	
2 $^2B_{3u}$	$\pi^*_{SOMO}-\pi^*$ - I	1.45	0.110	214.2	50.3	1.47, 1.53,[e] 1.48[f]
1 ^2A_u	$\pi^*_{SOMO}-\pi^*$ - I	1.82	0.001	256.0	92.1	
3 $^2B_{2u}$	$\pi^*_{SOMO}-\sigma^*$ - I	2.06	0.006	231.2	67.3	
2 $^2B_{3g}$	$\pi^*_{SOMO}-\sigma^*$ - I	2.09	fb	281.0	117.1	
3 $^2B_{3u}$	$\pi^*_{SOMO}-\pi^*$ - I	2.25	0.020	210.3	46.4	2.68, 2.66, ∼2.3[f]
4 ^2A_g	$\pi^*_{SOMO}-\sigma^*$ - I	2.27	fb	264.2	100.3	
3 $^2B_{1u}$	$\pi^*_{SOMO}-\sigma^*$ - I	2.38	fb	221.2	57.3	
4 $^2B_{3u}$	$\pi^*_{SOMO}-\pi^*$ - I	2.45	0.022	223.8	59.9	
3 $^2B_{2g}$	$\pi^*_{SOMO}-\pi^*$ - I	2.55	fb	269.6	105.7	
2 $^2B_{1g}$	$\pi^*_{SOMO}-\pi^*$ - I	2.74	fb	259.3	95.4	
5 ^2A_g	$\pi^*_{SOMO}-\sigma^*$ - I	2.97	fb	232.3	68.4	
6 ^2A_g	$\pi^*_{SOMO}-\sigma^*$ - I	3.08	fb	244.3	80.4	
4 $^2B_{2u}$	$\pi^*_{SOMO}-\sigma^*$ - I	3.12	0.000	265.2	101.3	
4 $^2B_{1u}$	$\pi^*_{SOMO}-\sigma^*$ - I	3.14	fb	258.1	94.2	
2 ^2A_u	$\pi-\pi^*_{SOMO}$ - II	3.24	0.089	169.5	5.6	3.35, 3.40, 3.19[f]
3 $^2B_{3g}$	$\pi^*_{SOMO}-\sigma^*$ - I	3.26	fb	242.9	79.0	
5 $^2B_{2u}$	$\pi^*_{SOMO}-\sigma^*$ - I	3.27	0.000	257.1	93.2	
5 $^2B_{1u}$	$\pi^*_{SOMO}-\sigma^*$ - I	3.34	fb	235.2	71.3	
3 ^2A_u	$\pi^*_{SOMO}-\pi^*$ - I	3.43	0.056	256.6	92.7	
4 $^2B_{2g}$	$\pi^*_{SOMO}-\pi^*$ - I	3.50	fb	234.8	70.9	
7 ^2A_g	$\pi^*_{SOMO}-\sigma^*$ - I	3.54	fb	221.9	58.0	
8 ^2A_g	$\pi^*_{SOMO}-\sigma^*$ - I	3.79	fb	230.4	66.5	
4 $^2B_{3g}$	$\pi^*_{SOMO}-\sigma^*$ - I	3.80	fb	238.2	74.3	
4 ^2A_u	$\pi^*_{SOMO}-v\pi^*$ - I	3.89	0.093	195.0	31.1	3.81
5 $^2B_{3u}$	$\pi^*_{SOMO}-\pi^*$ - I	4.13	0.021	210.5	46.6	
6 $^2B_{2u}$	$\pi^*_{SOMO}-\sigma^*$ - I	4.16	0.019	238.4	74.5	
6 $^2B_{1u}$	$\pi^*_{SOMO}-\sigma^*$ - I	4.28	fb	238.8	74.9	
5 $^2B_{3g}$	$\pi^*_{SOMO}-\sigma^*$ - I	4.40	fb	271.7	107.8	
7 $^2B_{2u}$	$\pi^*_{SOMO}-\sigma^*$ - I	4.45	0.012	230.8	66.9	
5 $^2B_{2g}$	$\pi^*_{SOMO}-\pi^*$ - I	4.54	fb	210.3	46.4	
9 ^2A_g	$\pi^*_{SOMO}-v\sigma^*$ - I	4.60	fb	193.5	29.6	
3 $^2B_{1g}$	$\pi^*_{SOMO}-\pi^*$ - I	4.67	fb	220.3	56.4	
6 $^2B_{3u}$	$\pi-\pi^*_{SOMO}$ - II[g]	4.84	0.343	203.2	39.3	4.20, 4.53[f]
10 ^2A_g	$\pi^*_{SOMO}-\sigma^*$ - I	5.14	fb	231.9	68.0	
7 $^2B_{1u}$	$\pi^*_{SOMO}-\sigma^*$ - I	5.22	fb	230.8	66.9	
6 $^2B_{3g}$	$\pi^*_{SOMO}-\sigma^*$ - I	5.28	fb	243.9	80.0	

[a]Reference 8 (in MTHF or *i*-BuNH$_2$) except for the values with notes. [b]Values in italic represent adiabatic electron affinities. [c]References 31 and 32. [d]Reference 33. [e]Reference 34. [f]Reference 35 (vertical value at the neutral geometry, gas phase). [g]To be accurate, $0.77(\pi-\pi^*_{SOMO}) + 0.80(\pi^*_{SOMO}-\pi^*)$.

calculated state includes two-electron process configurations with large coefficients, and its energy position is somewhat overestimated compared to that of the experimental one.

Despite the instability of the naphthalene anion, several experimental and theoretical studies have been reported.[35,76,79] In our calculations, a symmetry-forbidden state emerging from the anion ground state was calculated at 0.81 eV, which is assigned to shape-resonant $\pi^*_{SOMO}-v\pi^*$ ($^2B_{2g}$). This state corresponds to the experimentally observed states at ∼0.8 eV (on average),[34,35] and the assignment by Burrow et al.[35] based

dx.doi.org/10.1021/jp3051565 | J. Phys. Chem. A 2012, 116, 11833−11845

on ETS experiments and PPP calculations supports our interpretation. In the gas phase, electronic states were found at ~1.5, ~2.3, and ~3.2 eV. We expect that these naturally correspond to the first, second, and third bands in Figure 7, respectively. However, the assignments by Burrow et al.[35] are partly different from ours. Burrow et al. assigned the state at ~2.5 eV to ^2A_u, whereas it is $^2B_{3u}$ in our interpretation. In recent TDDFT calculations, excited states were found at ~1.5 and 2.4 eV above the anion ground state,[79] and their assignments are in accordance with ours. In ref 35, the state at ~3.1 eV was assigned to shape-resonant ^2A_u and $^2B_{2g}$ (note that it is $^2B_{1g}$ in the definition of the axes in the original article), whereas we assigned this state to a Feshbach resonance ^2A_u state. However, they also suggested that this state included considerable 2p1h (type II excitation) character, which is partially in accordance with our understanding. Furthermore, Burrow et al. found a state at 4.53 eV above the anion ground state and assigned it to $^2B_{2g}$ ($^2B_{1g}$ in the original article) which also included 2p1h character.[35] We associate this state with the fifth state in Figure 7 and assigned it to the $\pi-\pi^*_{SOMO}$ Feshbach resonance state ($^2B_{3u}$) including non-negligible shape-resonant $\pi^*_{SOMO}-v\pi^*$ character, although we do not think this interpretation is definitive.

5. COMPARISON BETWEEN CATION AND ANION RADICALS

The pairing theorem,[35,40−46] which is valid for alternant hydrocarbons within the Hückel and PPP-type theories, states that the π_n and π_n^* (n = 1, 2, ...) orbitals form pairs. It is capable of accounting for certain regularities in the π-orbital energies (which are associated with the IE and EA), $\pi-\pi^*$ transition energies, and spin density distributions on cations and anions of alternant hydrocarbons. If we set the zero-energy level at the midpoint of the HOMO−LUMO gap, the π_n and π_n^* orbitals have the same energies in absolute values. This indicates that the sum of the IE from the π_n orbital and the EA to the π_n^* orbital is a constant value.

Furthermore, the $\pi_m-\pi_n^*$ transition energy of the cation becomes identical to the $\pi_n-\pi_m^*$ transition energy of the anion. Figures 3, 4, and 7 show the pairing states in the excitation spectra of the three molecules. The $\pi-\pi_{SOMO}$ and $\pi_{SOMO}-\pi^*$ excited states of the cations correspond to the $\pi^*_{SOMO}-\pi^*$ and $\pi-\pi^*_{SOMO}$ states of the anions, respectively. If the cation and anion systems exactly satisfy the pairing theorem, the corresponding excitation spectra become equivalent. In fact, the pairing relationships are recognized between the spectral bands, although there is a somewhat energy shift and intensity difference in the spectra.

Table 9 shows the IE + EA values calculated by the SAC-CI method for the $\pi-\pi^*$ pair states of hexatriene, octatetraene, and naphthalene. The sums of the IEs from the π_{HOMO} states and EAs to the π^*_{LUMO} states for hexatriene, octatetraene, and naphthalene were calculated to be 7.54, 7.50, and 7.48 eV, respectively. These values are related to the ground-state energies of the cations and anions. The IE + EA values associated with the π_{HOMO-1} and π^*_{LUMO+1} states for hexatriene, octatetraene, and naphthalene were 8.12, 8.02, and 8.02 eV, respectively, which are derived from the energies of the lowest peaks in Figures 3, 4, and 7. These values are very similar. Furthermore, such similarity was also seen for the lowest non-Koopmans' states (dominated by two-electron processes from the neutral molecules), which correspond to the most intense peaks for hexatriene$^{\pm}$ and octatetraene$^{\pm}$ as

Table 9. IE + EA Values for $\pi-\pi^*$ Pair States of Hexatriene (HT), Octatetraene (OT), and Naphthalene (NA)[a]

π-π^* pair state	HT	OT	NA
(π_H^{-1})-(π^*_L)	7.54	7.50	7.48
(π_{H-1}^{-1})-(π^*_{L+1})	8.12	8.02	8.02
$(\pi_H^{-2}\,\pi^*_L)$-$(\pi_H^{-1}\,\pi^{*2}_L)$[b]	7.94	7.80	7.68

[a]Units in electronvolts. [b]The lowest non-Koopmans state.

well as the peaks at ~27 000 cm^{-1} for naphthalene$^{\pm}$. Their IE + EA values were 7.94, 7.80, and 7.68 eV, respectively, and were roughly constant.

These results indicate that the pairing theorem explains some features of the SAC-CI states of hexatriene$^{\pm}$, octatetraene$^{\pm}$, and naphthalene$^{\pm}$. On the other hand, note that the Hartree−Fock molecular orbitals with a large basis set do not satisfy the pairing theorem in contrast to the SAC-CI states. For example, the π^*_{LUMO+1} state is mainly described by the π^*_{LUMO+1} orbital but often consists of several non-negligible configurations other than the π^*_{LUMO+1} orbital. In this case, the orbital energies associated with the main configurations deviate from those expected from the pairing theorem.

6. SUMMARY

The excitation spectra of hexatriene cation/anion, octatetraene cation/anion, cyclopentadiene cation, 1,3-cyclohexadiene cation, and naphthalene cation/anion radicals were studied by the SAC-CI method, and the corresponding spectral bands were assigned. Although some of the calculated transition energies deviated somewhat from the corresponding experimental values, the SAC-CI results roughly reproduced the experimental spectra.

The spectra of all the cation radicals except naphthalene cation have two intense bands, whose lower band is assigned to the $\pi-\pi_{SOMO}$ transition and the upper one to the $\pi_{SOMO}-\pi^*$ transition. The four bands of the naphthalene cation are due to the $\pi-\pi_{SOMO}$, $\pi-\pi_{SOMO}$, $\pi_{SOMO}-\pi^*$, and $\pi_{SOMO}-\pi^*$ transitions, in order of increasing energy. The spectra of the cyclopentadiene and 1,3-cyclohexadiene cations are similar to that of *cis*-butadiene, indicating that these two molecules can be regarded as *cis*-butadiene analogs.

For the hexatriene and octatetraene anions, two bands are present, one of which is assigned to $\pi^*_{SOMO}-\pi^*$(diff) and the

dx.doi.org/10.1021/jp3051565 | J. Phys. Chem. A 2012, 116, 11833−11845

other to $\pi-\pi^*_{SOMO}$, in order of increasing energy. Intense bands for the naphthalene anion originate from $\pi^*_{SOMO}-\pi^*$(diff), $\pi^*_{SOMO}-\pi^*$(diff), $\pi-\pi^*_{SOMO}$, $\pi^*_{SOMO}-v\pi^*$, and $\pi-\pi^*_{SOMO}$, also in order of increasing energy. The SAC-CI calculations of a model solute−solvent complex, the hexatriene anion sandwiched between the point charges expressing two MTHF molecules, indicated that the solvent effect on the spectrum was small.

The IEs and EAs of the target molecules were also calculated and were found to be in good agreement with the corresponding experimental values. The EA of octatetraene was predicted to be positive, suggesting that the crossover from negative to positive EAs in the linear polyenes occurs between hexatriene and octatetraene. The IE + EA values of hexatriene, octatetraene, and naphthalene were almost constant for their three $\pi-\pi^*$ pairing states. Therefore, the pairing theorem explains some features of the SAC-CI results for hexatriene, octatetraene, and naphthalene cations/anions.

■ ASSOCIATED CONTENT

Supporting Information

Detailed tables presenting the electronic ground and excited states (Tables S1−S8), the molecular orbital information (Tables S9−S12), and molecular geometries (Tables S13−S16) for the eight target cation/anion radicals. This material is available free of charge via the Internet at http://pubs.acs.org.

■ AUTHOR INFORMATION

Corresponding Author

*Tel & Fax: +81-75-634-3211. E-mail: h.nakatsuji@qcri.or.jp.

Present Address

[‖]West-Japan Division, HPC SYSTEMS, Inc., 646 Karasuma-dori-Ayanokoji-kudaru, Shimogyo-ku, Kyoto 600−8412, Japan. Tel: +81-75-353-0120. Fax: +81-75-353-0121. E-mail: ya-honda@hpc.co.jp

Notes

The authors declare no competing financial interest.

■ REFERENCES

(1) Hudson, B. S.; Kohler, B. E.; Schulten, K. In *Excited States*; Lim, E. C., Ed.; Academic Press: New York, 1982; Vol. *6*, p 1.

(2) (a) Salama, F.; Allamandola, L. J. *Astrophys. J.* **1992**, *395*, 301−306. (b) Salama, F.; Allamandola, L. J. *Adv. Space Res.* **1995**, *15*, 413−422.

(3) Weisman, J. L.; Lee, T. J.; Salama, F.; Head-Gordon, M. *Astrophys. J.* **2003**, *587*, 256−261.

(4) Curl, R. F. *Nature* **1993**, *363*, 14−15.

(5) Pope, C. J.; Marr, J. A.; Howard, J. B. *J. Phys. Chem.* **1993**, *97*, 11001−11013.

(6) Harvey, R. G. *Polycyclic Aromatic Hydrocarbons: Chemistry and Carcinogenesis*; Cambridge University Press: Cambridge, U.K., 1991.

(7) Rehwagen, M.; Müller, A.; Massolo, L.; Herbarth, O.; Ronco, A. *Sci. Total Environ.* **2005**, *348*, 199−210.

(8) Shida, T. *Physical Sciences Data 34 "Electronic absorption spectra of radical ions"*; Elsevier: Amsterdam, 1988.

(9) Eland, J. H. D. *Photoelectron Spectroscopy*; John Wiley & Sons: New York, 1974.

(10) Rabalais, J. W. *Principles of Ultraviolet Photoelectron Spectroscopy*; John Wiley & Sons: New York, 1977.

(11) Jordan, K. D.; Burrow, P. D. *Acc. Chem. Res.* **1978**, *11*, 341−348.

(12) Gavin, R. M., Jr.; Rice, S. A. *J. Chem. Phys.* **1974**, *60*, 3231−3237.

(13) Beez, M.; Bieri, G.; Bock, H.; Heilbronner, E. *Helv. Chim. Acta* **1973**, *56*, 1028−1046.

(14) Bally, T.; Nitsche, S.; Roth, K.; Haselbach, E. *J. Am. Chem. Soc.* **1984**, *106*, 3927−3933.

(15) Dunbar, R. C.; Teng, H. H.-I. *J. Am. Chem. Soc.* **1978**, *100*, 2279−2283.

(16) Jones, T. B.; Maier, J. P. *Int. J. Mass Spectrosc. Ion Phys.* **1979**, *31*, 287−291.

(17) Kiselev, V. D.; Sakhabutdinov, A. G.; Shakirov, I. M.; Zverev, V. V.; Konovalov, A. I. *Zh. Org. Khim.* **1992**, *28*, 2244−2252.

(18) Kimura, K.; Katsumata, S.; Achiba, Y.; Yamazaki, T.; Iwata, S. *Handbook of HeI Photoelectron Spectra of Fundamental Organic Compounds*; Japan Scientific Soc. Press: Tokyo, 1981.

(19) Cockett, M. C. R.; Ozeki, H.; Okuyama, K.; Kimura, K. *J. Chem. Phys.* **1993**, *98*, 7763−7772.

(20) Gotkis, Y.; Oleinikova, M.; Naor, M.; Lifshitz, C. *J. Phys. Chem.* **1993**, *97*, 12282−12290.

(21) Bally, T.; Carra, C.; Fülscher, M. P.; Zhu, Z. *J. Chem. Soc., Perkin Trans. 2* **1998**, 1759−1765.

(22) Halasinski, T. M.; Salama, F.; Allamandola, L. J. *Astrophys. J.* **2005**, *628*, 555−566.

(23) Brechignac, P.; Pino, T.; Boudin, N. *Spectrochim. Acta* **2001**, *57*, 745−756.

(24) Pino, T.; Boudin, N.; Bréchignac, P. *J. Chem. Phys.* **1999**, *111*, 7337−7347.

(25) Romanini, D.; Biennier, L.; Salama, F.; Kachanov, A.; Allamandola, L. J.; Stoeckel, F. *Chem. Phys. Lett.* **1999**, *303*, 165−170.

(26) Biennier, L.; Salama, F.; Gupta, M.; O'Keefe, A. *Chem. Phys. Lett.* **2004**, *387*, 287−294.

(27) Kelsall, B. J.; Andrews, L. *J. Chem. Phys.* **1982**, *76*, 5005−5013.

(28) Salama, F.; Allamandola, L. J. *J. Chem. Phys.* **1991**, *94*, 6964−6977.

(29) Burrow, P. D.; Jordan, K. D. *J. Am. Chem. Soc.* **1982**, *104*, 5247−5248.

(30) Allan, M.; Neuhaus, L.; Haselbach, E. *Helv. Chim. Acta* **1984**, *67*, 1776−1782.

(31) Lyapustina, S. A.; Xu, S. K.; Nilles, J. M.; Bowen, K. H. *J. Chem. Phys.* **2000**, *112*, 6643−6648.

(32) Schiedt, J.; Knott, W. J.; Le Barbu, K.; Schlag, E. W.; Weinkauf, R. *J. Chem. Phys.* **2000**, *113*, 9470−9478.

(33) Song, J. K.; Han, S. Y.; Chu, I. H.; Kim, J. H.; Kim, S. K.; Lyapustina, S. A.; Xu, S. J.; Nilles, J. M.; Bowen, K. H. *J. Chem. Phys.* **2002**, *116*, 4477−4481.

(34) Hoytink, G. J. *Chem. Phys. Lett.* **1974**, *26*, 318−322.

(35) Burrow, P. D.; Michejda, J. A.; Jordan, K. D. *J. Chem. Phys.* **1987**, *86*, 9−24.

(36) Allan, M. *Helv. Chim. Acta* **1982**, *65*, 2008−2023.

(37) Brandes, K. K.; Gerdes, R. J. *J. Phys. Chem.* **1967**, *71*, 508−513.

(38) Compton, R. N.; Huebner, R. H.; Reinhardt, P. W.; Christophorou, L. G. *J. Chem. Phys.* **1968**, *48*, 901−909.

(39) Koopmans, T. *Physica* **1934**, *1*, 104−113.

(40) Staley, S. W.; Strnad, J. T. *Chem. Phys. Lett.* **1992**, *200*, 527−533.

(41) Salem, L. *The Molecular Orbital Theory of Conjugated Systems*; Benjamin: New York, 1966.

(42) Coulson, C. A.; Rushbrooke, G. S. *Proc. Cambridge Philos. Soc.* **1940**, *36*, 193−200.

(43) McLachlen, A. D. *Mol. Phys.* **1961**, *4*, 49−56.

(44) Koutecky, J. *J. Chem. Phys.* **1966**, *44*, 3702−3706; **1967**, *47*, 1501−1511.

(45) Longuet-Higgins, H. C.; Pople, J. A. *Proc. Phys. Soc. A* **1955**, *68*, 591−600.

(46) Mayer, I. *Mol. Phys.* **2010**, *108*, 3273−3278.

(47) Nakatsuji, H.; Hirao, K. *J. Chem. Phys.* **1978**, *68*, 2053−2065.

(48) Nakatsuji, H. *Chem. Phys. Lett.* **1978**, *59*, 362−364.

(49) Nakatsuji, H. *Chem. Phys. Lett.* **1979**, *67* (329−333), 334−342.

(50) Nakatsuji, H. *Acta Chim. Hung.* **1992**, *129*, 719−776.

(51) Nakatsuji, H. *Computational Chemistry, Reviews of Current Trends*; Leszczynski, J., Ed.; World Scientific: Singapore, 1997; Vol. 2.

(52) Ehara, M.; Ishida, M.; Nakatsuji, H. *J. Chem. Phys.* **2002**, *117*, 3248−3255.

(53) Ehara, M.; Yasuda, S.; Nakatsuji, H. *Z. Phys. Chem.* **2003**, *217*, 161−176.
(54) Kuramoto, K.; Ehara, M.; Nakatsuji, H. *J. Chem. Phys.* **2005**, *122*, 014304.
(55) Ehara, M.; Ohtsuka, Y.; Nakatsuji, H.; Takahashi, M.; Udagawa, Y. *J. Chem. Phys.* **2005**, *122*, 234319.
(56) Fujimoto, K.; Hasegawa, J.; Hayashi, S.; Nakatsuji, H. *Chem. Phys. Lett.* **2006**, *432*, 252−256.
(57) Hasegawa, J.; Bureekaew, S.; Nakatsuji, H. *J. Photochem. Photobiol. A: Chem.* **2007**, *189*, 205−210.
(58) Hasegawa, J.; Fujimoto, K.; Swerts, B.; Miyahara, T.; Nakatsuji, H. *J. Comput. Chem.* **2007**, *28*, 2443−2452.
(59) Nakatani, N.; Hasegawa, J.; Nakatsuji, H. *J. Am. Chem. Soc.* **2007**, *129*, 8756−8765.
(60) Fujimoto, K.; Hasegawa, J.; Nakatsuji, H. *Chem. Phys. Lett.* **2008**, *462*, 318−320.
(61) Fujimoto, K.; Hasegawa, J.; Nakatsuji, H. *Bull. Chem. Soc. Jpn.* **2009**, *82*, 1140−1148.
(62) Miyahara, T.; Nakatsuji, H.; Hasegawa, J.; Osuka, A.; Aratani, N.; Tsuda, A. *J. Chem. Phys.* **2002**, *117*, 11196−11207.
(63) Hasegawa, J.; Takata, K.; Miyahara, T.; Neya, S.; Frisch, M. J.; Nakatsuji, H. *J. Phys. Chem. A* **2005**, *109*, 3187−3200.
(64) Nakatsuji, H.; Matsumune, N.; Kuramoto, K. *J. Chem. Theor. Comp.* **2005**, *1*, 239−247.
(65) Honda, Y.; Hada, M.; Ehara, M.; Nakatsuji, H. *J. Phys. Chem. A* **2002**, *106*, 3838−3849.
(66) Honda, Y.; Hada, M.; Ehara, M.; Nakatsuji, H. *J. Phys. Chem. A* **2007**, *111*, 2634−2639.
(67) Dunning, T. H., Jr. *J. Chem. Phys.* **1970**, *53*, 2823−2833.
(68) Dunning, T. H., Jr.; Hay, P. J. *Modern Theoretical Chemistry*; Schaefer, H. F., III, Ed.; Plenum Press: New York, 1977; Vol. 3.
(69) Frisch, M. J.; Trucks, G. W.; Schlegel, H. B.; Scuseria, G. E.; Robb, M. A.; Cheeseman, J. R.; Scalmani, G.; Barone, V.; Mennucci, B.; Petersson, G. A.; Nakatsuji, H.; et al. *Gaussian 09*, Revision B.01; Gaussian, Inc.: Wallingford, CT, 2010.
(70) Nakatsuji, H. *Chem. Phys.* **1983**, *75*, 425−441.
(71) SAC-CI GUIDE, http://www.qcri.or.jp/sacci/.
(72) Fukuda, R.; Nakatsuji, H. *J. Chem. Phys.* **2008**, *128*, 094105.
(73) Nakatsuji, H. *Chem. Phys. Lett.* **1991**, *177*, 331−337.
(74) Ehara, M.; Ishida, M.; Toyota, K.; Nakatsuji, H. In *Reviews in Modern Quantum Chemistry (A tribute to Professor Robert G. Parr)*; Sen, K. D., Ed.; World Scientific: Singapore, 2003; pp 293−319.
(75) Fülscher, M. P.; Matzinger, S.; Bally, T. *Chem. Phys. Lett.* **1995**, *236*, 167−176.
(76) Carsky, P.; Zahradnik, R. *Theor. Chim. Acta* **1970**, *17*, 316−319.
(77) Hirata, S.; Lee, T.; Head-Gordon, M. *J. Chem. Phys.* **1999**, *111*, 8904−8912.
(78) Malloci, G.; Mulas, G.; Joblin, C. *Astron. Astrophys.* **2004**, *426*, 105−117.
(79) Malloci, G.; Mulas, G.; Cappellini., G.; Joblin, C. *Chem. Phys.* **2007**, *340*, 43−58.
(80) Löwdin, P.-O. *J. Math. Phys.* **1962**, *3*, 969−982.
(81) Taylor, H. S. *Adv. Chem. Phys.* **1970**, *18*, 91−147.
(82) Simons, J.; Jordan, K. D. *Chem. Rev.* **1987**, *87*, 535−555.
(83) Reisler, H.; Krylov, A. I. *Int. Rev. Phys. Chem.* **2009**, *28*, 267−308.